Journal of Hydro-environment Research 19 (2018) 214–223

Contents lists available at ScienceDirect

Journal of Hydro-environment Research

journal homepage: www.elsevier.com/locate/JHER

Alternative mitigation measures for fish passage in standard box culverts: Physical modelling

Hang Wang, Warren Uys, Hubert Chanson *

The University of Queensland, School of Civil Engineering, Brisbane, QLD 4072, Australia

ARTICLE INFO

Article history:
Available online 4 April 2017

Keywords:
Standard box culvert
Small-bodied fish passage
Baffles
Rough boundaries
Secondary currents
Physical modelling

ABSTRACT

Road crossings and culverts are common man-made structures along river courses, ranging from national highways to rural roads and urban networks. Present expertise in culvert hydraulic design is deficient because many empirically-based guidelines are often inadequate for fish passage. This project focused on the development of simple solutions for box culverts, with the aim to maximise slow flow regions suitable for small-bodied fish passage and to minimise the reduction in discharge capacity. Herein a physical study of box culvert was performed under controlled flow conditions, and seven designs were tested. In all the cases, the turbulence of the flowing waters was used to assist with fish migration. One baffle configuration presented promising results: i.e., small corner baffles. The triangular baffle system produced little additional afflux, while creating excellent recirculations both upstream and downstream of each baffle. Another configuration was based upon a rough bed and sidewall, enhancing secondary currents and recirculation in the corner region. This resulted in flow conditions that could be potentially used to enhance small-bodied fish passage, though further experiments involving detailed fish behaviour study are required for quantitative guidelines.

1. Introduction

Culverts are road crossings designed to pass floodwaters beneath a roadway embankment. Culvert designs are diverse, using various shapes and materials determined by stream width, peak flows, stream gradient, and minimum cost (Henderson, 1966; Hee, 1969; Chanson, 2004). While the key design parameters of a culvert are its design discharge and the maximum acceptable afflux, the variability in culvert dimensions is linked to the characteristics and constraints of the site where the road crossing has to be built (Fig. 1). This variability results in a wide diversity in flow patterns that can be observed in existing culverts. Fig. 1 presents a few examples of small to large standard box culverts in Australia. The two-cell structure seen in Fig. 1 (Top Left) would be typical of a large majority of road culvert structures.

For the past few decades, concerns regarding the ecological impact of culvert crossings have led to changes in their design. Although the overall culvert discharge capacity is based upon hydrological and hydraulic engineering considerations, large flow velocities may create a fish passage barrier. In some cases, the environmental impact on fish passage may affect the upstream catchment with adverse impact on the stream ecology, because the installation of road crossings can limit the longitudinal connectivity of streams for fish movement (Warren and Pardew, 1998; Brigg and Galarowicz, 2013). Common fish passage barriers include excessive vertical drop at the culvert outlet (perched outlet), high velocity or inadequate flow depth within the culvert barrel, excessive turbulence, and debris accumulation at the culvert inlet (Olsen and Tullis, 2013). The increased velocities in the barrel can produce reduced flow depths, potentially inadequate for fish passage, relative to the culvert size. Higher culvert exit velocities may also increase perched outlet fall heights (fish barrier) with increased scour hole development downstream.

For culvert rehabilitation applications where fish passage may be a concern, baffles installed along the invert may provide a more fish-friendly alternative, albeit the discharge capacity may be adversely reduced (Larinier, 2002; Olsen and Tullis, 2013). A recent discussion paper recommended that three-dimensional analysis of culvert flows should be considered to gain an understanding of the turbulence and secondary flow motion (Papanicolaou and Talebbeydokhti, 2002). It recommended an in-depth examination of the spanwise and vertical velocity distributions as well as turbulent intensities and kinetic energy, in view of the importance of these parameters to fish passage.

* Corresponding author.
E-mail address: h.chanson@uq.edu.au (H. Chanson).

http://dx.doi.org/10.1016/j.jher.2017.03.001

List of symbols

B	channel width (m)
D_H	hydraulic diameter (m)
d	water depth (m)
d_{tw}	tailwater depth (m)
f	Darcy-Weisbach friction factor
H	internal channel height (m)
k_s	equivalent sand roughness height
L	channel length (m)
Q	water discharge (m^3/s)
Q_{des}	design discharge (m^3/s)
Re	Reynolds number defined in terms of bulk velocity and hydraulic diameter: $Re = V_{mean} \times DH/\nu$
S_o	bed slope
V	velocity component (m/s)
V_{fs}	longitudinal velocity (m/s) at the free-surface
V_{max}	maximum longitudinal velocity (m/s) at a transverse location y
V_{mean}	cross-sectional averaged velocity (m/s): $V_{mean} = Q/(B \times d)$
v′	velocity component standard deviation (m/s)
x	longitudinal coordinate (m)
Y_{Vmax}	transverse location (m) where the cross-section maximum longitudinal velocity is observed
y	transverse coordinate (m) measured from the right sidewall
Z_{Vmax}	vertical elevation (m) where the maximum longitudinal velocity V_{max} is observed
z	vertical elevation (m)
Δh	afflux (m)
ν	kinematic viscosity (m^2/s)

Subscript

des	culvert design flow conditions
max	maximum value
min	minimum value
tw	tailwater conditions
x	longitudinal componet
y	transverse component
z	vertical component

Fig. 1. Photographs of standard multi-cell box culverts in Australia – Top Left: damaged box culvert in the Condamine River catchment on 5 Jan. 2011; Top Right: Culvert outlet in Algester, Brisbane in Aug. 1999; Bottom: Culvert on Gin House Creek, Gold Coast on 5 Dec. 2007.

The selection of the type of culvert fish pass and of the fish pass characteristics depends on the swimming capacities of the fish species. Currently there was no simple technical means for measuring the characteristics of turbulence in a fish pass, although it is acknowledged that the turbulence in a fish pass plays a key role in fish behaviour (Liu et al., 2006; Yasuda, 2011; Breton et al., 2013). Key turbulence characteristics, deemed most important to fish movement, were identified as turbulence intensity, Reynolds stresses, turbulent kinetic energy, vorticity, dissipation and eddy length scales (Pavlov et al., 2000; Hotchkiss, 2002; Nikora et al., 2003; Webb and Cotel, 2011). Recent observations showed that fish may further take advantage of the unsteady character of the turbulent flow (Liao et al., 2003; Wang et al., 2010).

The present investigation was motivated by the needs to facilitate upstream passage of small-bodied Australian native fish species in box culverts. With such fish species, the adults have typically a total length less than 150 mm and sprint/burst speed less than 0.6 m/s. Current Australia national guidelines for

small-bodied fish species suggest that water depth should range between 0.2 and 0.5 m with bulk velocity less than 0.3 m/s during base flows (Fairfull and Witheridge, 2003), thus yielding uneconomical culvert designs. In this paper, physical testing of a range of design configurations for standard box culvert was conducted. Physical modelling was conducted in laboratory under controlled flow conditions to test seven designs, with the aim to minimise the afflux increase and to maximise slow flow, secondary current and recirculation regions suitable to small-bodied fish passage. The project focused on the development of simple solutions, which could be used for new designs as well as to retrofit existing box culverts.

2. Experimental facility and flow conditions

2.1. Presentation

Two series of physical tests were conducted in Froude models. The first series was conducted in a box culvert model with a focus on baffle designs (Fig. 2). The model was installed in a 1 m wide flume and the culvert barrel's internal dimensions were: B = 0.150 m, H = 0.105 m, L = 0.50 m where B is the internal width, H is the internal height, and L is the length of the barrel. The barrel invert was aligned with the upstream and downstream channel bed. The design flow conditions of the culvert model were: Q_{des} = 0.010 m^3/s and Δh = 0.087 m, where Δh is the afflux, for a tailwater depth d_{tw} = 0.038 m.

The second series of experiments was conducted in a tilting flume, to document secondary currents in the presence of boundary roughness (Fig. 3). The channel was 12 m long 0.5 m wide and the bed slope was horizontal herein. The flume was made of smooth PVC bed and glass walls. The waters were supplied by a constant head tank feeding a large intake basin (2.1 m long, 1.1 m wide, 1.1 m deep) leading to the flume through a series of flow straighteners, followed by a bottom and sidewall convergent, delivering smooth and quasi-uniform inflow conditions.

In both facilities, water was supplied from a constant head tank. The discharge was measured by a flow meter calibrated on site. Free-surface measurements were performed using a pointer gauge. Detailed velocity measurements were conducted in the 12 m long flume using an acoustic Doppler velocimeter (ADV) Nortek™ Vectrino+ equipped with a three-dimensional side-looking head. The velocity range was ±1.0 m/s and the ADV signal was sampled at 200 Hz for 180 s at each point. The translation of the ADV probe in the vertical direction was controlled by a fine adjustment travelling mechanism connected to a Mitutoyo™ digimatic scale unit. The error on the vertical position of the probes was $\Delta z < 0.025$ mm. The accuracy on the longitudinal position was estimated as $\Delta x < \pm 2$ mm. The accuracy on the transverse position of the probe was less than 1 mm.

2.2. Boundary conditions

During the first series of experiments, six baffle designs were tested, in addition to a smooth (reference) configuration (Fig. 2B, Table 1). The corner baffle design and both diagonal baffle designs aimed to generate recirculation in the barrel. The rough inverts were designed to reduce locally the velocity next to the invert. The 'partial pipe' configuration was designed to maximise the wetted perimeter and to increase locally the boundary roughness effects. The system was not applied to the full barrel length, hence the term 'partial', to reduce the risk of debris clogging.

The corner baffle system consisted of triangular baffles fixed in the bottom left corner of the barrel. Each triangular baffle was 0.02 m high and wide, and a baffle was positioned every 0.10 m. The most upstream baffle was positioned 0.05 m inside the barrel, and the most downstream baffle was positioned 0.05 m before the barrel outlet. The partial pipe design consisted of rectangular plates, 0.05 m by 0.03 m, fixed diagonally at 45°. Seven plates were installed, with a gap of 0.025 m between plates. The first plate was fixed with its leading edge in line with the barrel entrance. Gaps between rectangular plates were introduced to avoid fish traveling through complete darkness since fish tend to be attracted to regions of light (Breton et al., 2013). The diagonal baffle configuration consisted of 0.012 m high baffles, oriented to 60° with the streamwise flow direction, with 0.10 m longitudinal spacing between baffles. The leading edge of the most upstream baffle was located 0.0125 m inside the barrel. Each baffle was positioned with a 0.01 m gap between the barrel sidewalls and the baffles to prevent debris clogging. The streamlined diagonal baffle design was based upon the diagonal baffles, with a 30° ramp installed upstream of each baffle to reduce the energy loss.

For the second series of experiments in the 12 m long flume, two boundary configurations were tested. One had the original smooth bed and glass sidewalls. The second consisted of a rough bed, a rough sidewall and a smooth sidewall (Fig. 3). The rubber mats consisted of square patterns: 0.0482 m × 0.0482 m for the bed, and 0.0375 m × 0.0375 m for the left sidewall. In line with d-type roughness studies (Djenidi et al., 1999), the vertical elevation z was measured at the top of the mats and this was supported by visual observations suggesting zero to negligible flow motion through the mats themselves. The hydraulic roughness was tested for a range of steady flow conditions. The boundary shear stress was deduced from measured free-surface profiles and estimated friction slopes. For the rough bed and sidewall configuration, the equivalent Darcy-Weisbach friction factor was f = 0.07–0.12, corresponding to an 'equivalent' sand roughness height 20 mm < k_s < 30 mm. In comparison, the Darcy-Weisbach friction factor f for the smooth boundary configuration ranged from 0.015 to 0.017, corresponding to a mean equivalent sand roughness height $k_s \approx 0.2$ mm.

2.3. Experimental modelling and flow conditions

Most hydraulic structure models are scaled down using an undistorted geometric similarity assuming implicitly a Froude similitude (ASCE, 1942; Henderson, 1966). When the same fluids, air and water herein, are used in model and prototype, a Morton similitude is achieved and the Reynolds number is drastically underestimated in the laboratory model (Novak and Cabelka, 1981; Pfister and Chanson, 2012). The model flow must be turbulent and the Reynolds number must satisfy: $Re > 1 \times 10^3$ to 5×10^3 (Henderson, 1966; Novak et al., 2001; Chanson, 1999).

For the first series, tests were conducted for eight flow rates between Q = 0.001 m^3/s and 0.014 m^3/s corresponding to $2.2 \times 10^4 < Re < 1.6 \times 10^5$, with Re the Reynolds number of the barrel flow. For each flow rate, three tailwater water depths were tested: i.e., 0.020 m, 0.038 m and 0.045 m. For Q > 0.014 m^3/s, the embankment became overtopped. Visual observation of flow recirculation and turbulence was conducted by injecting vegetable dye around points of interest. Photographs and video movies were taken to characterise the slow flow motion and recirculation regions. The afflux was also recorded.

During the second series of tests, velocity measurements were performed for two discharges at several longitudinal locations (0.65 m < x < 10 m) and at several transverse locations y, with y = 0 at the right glass sidewall. The flow conditions corresponded to $1.4 \times 10^5 < Re < 2.5 \times 10^5$ (Table 1). Preliminary measurements indicated that the flow became fully-developed for x > 6.5–8 m on the smooth bed configuration (Wang et al., 2016). With the rough bed and sidewall configuration, both sidewall and bed

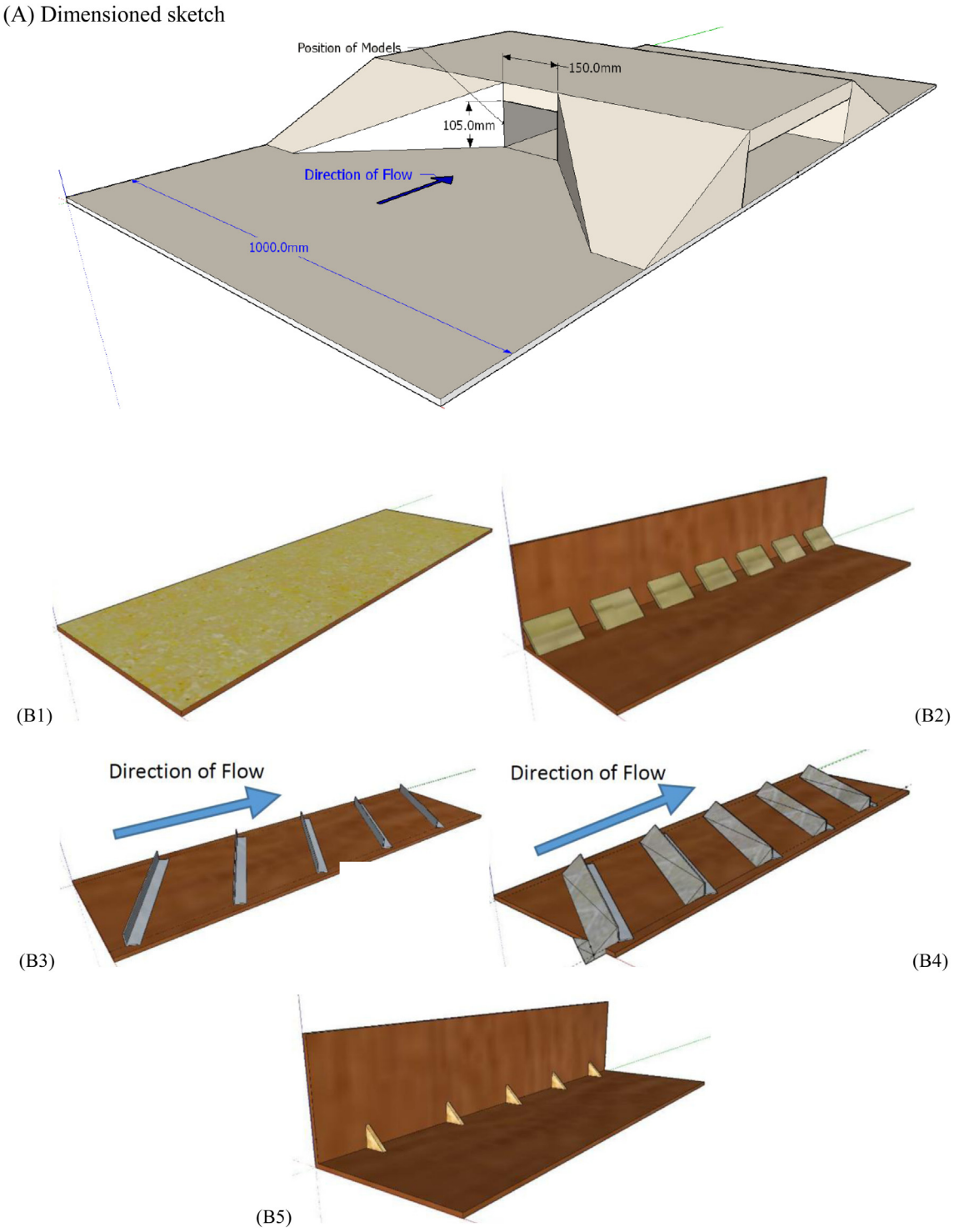

Fig. 2. Box culvert model and baffle designs. (A) Dimensioned sketch. (B) Baffle designs – From top to bottom, left to right: rough sand paper, partial pipe system, diagonal baffles, streamlined diagonal baffles and corner triangular baffles.

boundary layer developments were observed together with strong interactions between the two boundary layer processes. The velocity data suggested that the flow was fully-three-dimensional for $x > 4$ m.

Table 1 summarises the experimental flow conditions. Note that all investigated flow conditions operated with Reynolds numbers one to two orders of magnitude larger than the recommended guidelines. Further, in Eastern Australia, about 90% of road culverts are less than 10 m long and a large majority have one or two cells, typically less than 1 m wide (internal cell width). Herein the small model (series 1) may be regarded as a 1:6 to 1:3 scale model of a typical single-cell road culvert, while the 12 m long 0.5 m wide channel (series 2) is a near full-scale single-cell culvert barrel structure. It is acknowledged that the extrapolation of the small box culvert results to full-scale might require further validation, while the experiments in the 0.5 m wide tilting flume may be capable to reproduce prototype turbulence characteristics within a reasonable extent.

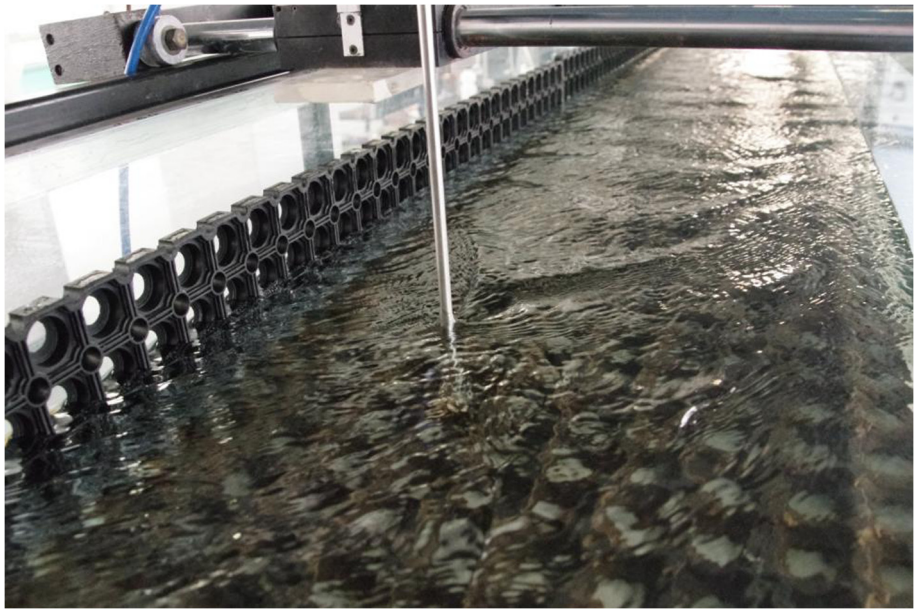

Fig. 3. Long channel with rough bed and rough sidewall – Flow conditions: Q = 0.026 m^3/s, flow direction from left to right.

Table 1
Experimental flow conditions (present study).

Exp.	S_o	B m	Q m^3/s	V_{mean} m/s	Re	Boundary conditions	Remarks
Series 1	0	0.150	0.001 to 0.014	0.05 to 0.97	2.2×10^4 to 1.6×10^5	Smooth barrel Grade P40 sandpaper ($k_s \approx 0.43$ mm ([1])) Grade P60 sandpaper ($k_s \approx 0.27$ mm ([1])) Corner baffles (0.02 m × 0.02 m, 0.10 m apart) Partial pipe Diagonal baffles (0.012 m high, 60°) Streamlined diagonal baffles (0.012 m high, 60°)	Box culvert
Series 2	0	0.50	0.0261 0.0556	0.44 0.59	1.4×10^5 to 2.5×10^5	PVC bed & glass sidewalls	12 m long flume
		0.478	0.0261 0.0556	0.38 0.58	1.4×10^5 to 2.5×10^5	Rough bed, rough left sidewall, glass right sidewall	

Notes: B: channel width; Q: water discharge; Re: Reynolds number defined in terms of hydraulic diameter; S_o: bed slope; V_{mean}: cross-section average velocity; ([1]): Washington Mills (2015).

3. Culvert baffle hydraulics

3.1. Flow patterns and recirculation

In the culvert model (Series 1), the basic flow patterns were investigated systematically for all discharges and tailwater levels. This section summarises the key outcomes. The rough invert (sand paper) configurations slowed the fluid velocity in the very close vicinity of the barrel invert. The effect of the P40 sandpaper was greater than that of the P60 sandpaper. In both cases, their effect was restricted to a very thin layer of fluid immediately above the invert (Fig. 4A). With the partial pipe system, the decrease in velocity did not appear to be significant when compared to the variability in flow velocity across the barrel (Fig. 4B). Combined with a lack of flow recirculation, the design was deemed not practical for fish passage.

The diagonal baffle design had different impacts depending upon the discharge. At low flows, the design caused a hydraulic drop immediately downstream of the last baffle, which could be an obstacle for fish passage. At larger flows, the diagonal baffles created regions of helicoidal recirculation (Fig. 4C). Although these could act as resting spots for fish, it is unknown which fish species could take advantage of such a recirculation motion. Practically the diagonal baffle system had the potential to cause a debris build-up within the barrel. The effectiveness of the diagonal baffle system was improved by the installation of a ramp in front of each baffle. The ramp reduced the drag caused by a baffle and may reduce the build-up of debris due to the flow streamlining.

In the corner baffle configuration, recirculation eddies were observed between baffles. Each triangular baffle caused recirculation zones extending both upstream and downstream (Fig. 4D). For the selected baffle dimensions, the spacing between baffles allowed the upstream and downstream recirculation zones to connect. The patterns of these recirculation zones were close to those described by Liu et al. (2006) in vertical slot fishways. Overall the corner baffles generated recirculation currents that could allow small fish to rest between episodes of burst speed or sustained speed swimming (Baker and Votapka, 1990).

3.2. Relationship between afflux and discharge

For a range of flow conditions, the relationship between discharge and afflux was investigated for all designs including the un-modified box culvert. Fig. 5 presents the results, with the solid

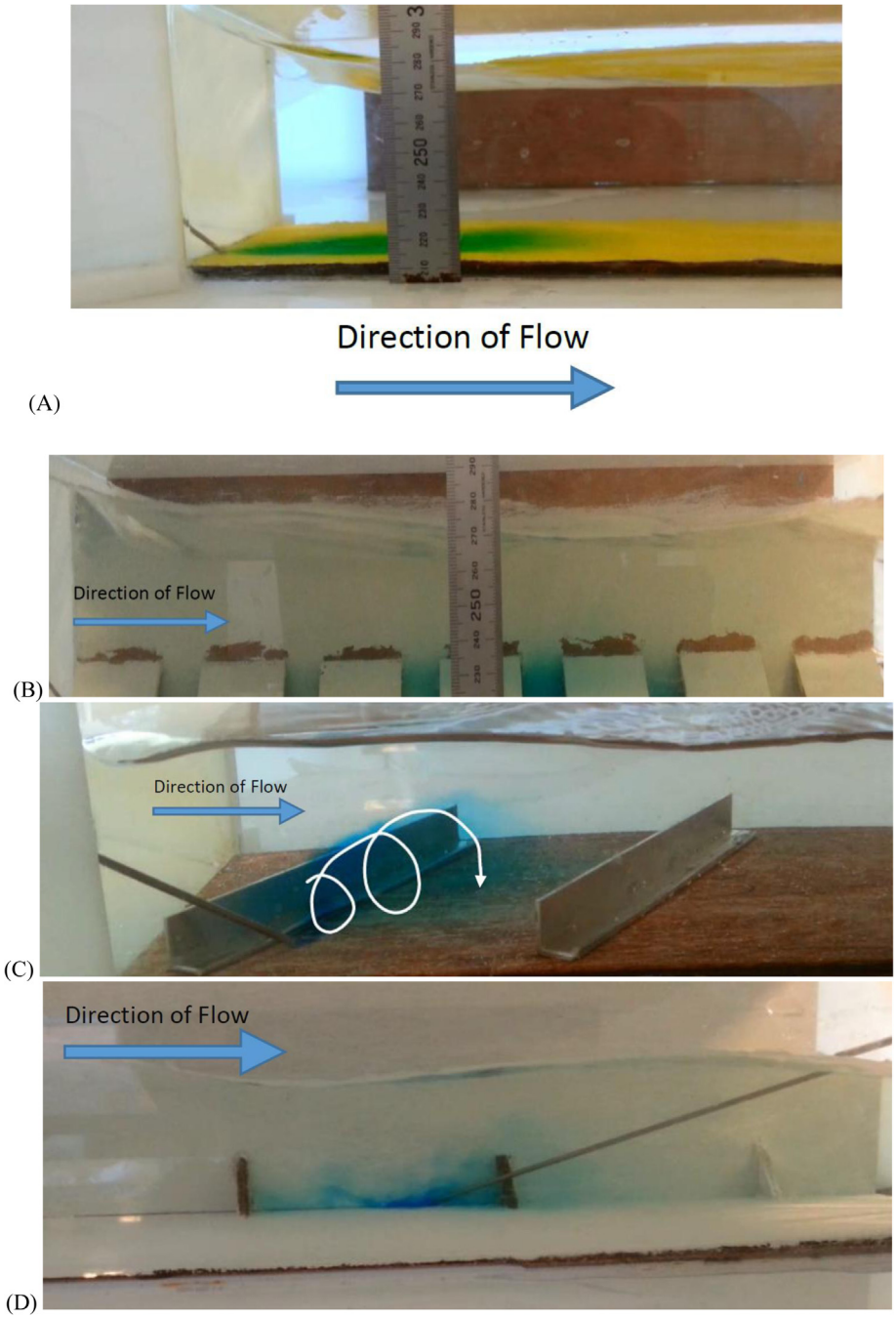

Fig. 4. Photographs of slow flow and recirculation regions in the culvert barrel highlighted using dye injection – Flow direction from left to right.

vertical line highlighting the design flow conditions. Namely a culvert structure is designed for a design discharge Q_{des}, and maximum acceptable afflux, for which the culvert dimensions are optimised (Henderson, 1966; Chanson, 1999). The culvert performed under inlet control for flow rates above $Q \geq 0.0035$ m^3/s. At low flow rates the culvert operated as outlet control. That is, the upstream water height was a function of tailwater depth. Typical results in terms of the relationship between afflux and discharge are presented in Fig. 5. Overall the rough sand paper invert designs, corner baffle design and partial pipe design yielded the smallest increase in afflux for a given discharge and tailwater level. The largest increase in afflux was observed with the diagonal baffle design for all flow conditions, with an increase in afflux of 0.01–0.02 m: i.e., 20–50% increase in afflux depending upon the discharge (Fig. 5). Note that the streamlined diagonal baffle design yielded intermediate results, albeit slightly larger afflux than for the diagonal baffle design with $Q > 0.009$ m^3/s. This was caused by differences barrel flow regimes, with the diagonal baffle culvert operating into drowned conditions for $Q > 0.009$ m^3/s (Chanson and Uys, 2016).

The results enabled to deduce the reduction in discharge capacity for a given afflux. For example, at design flow conditions, the corner baffle design yielded a 10% reduction in maximum discharge capacity (Fig. 5).

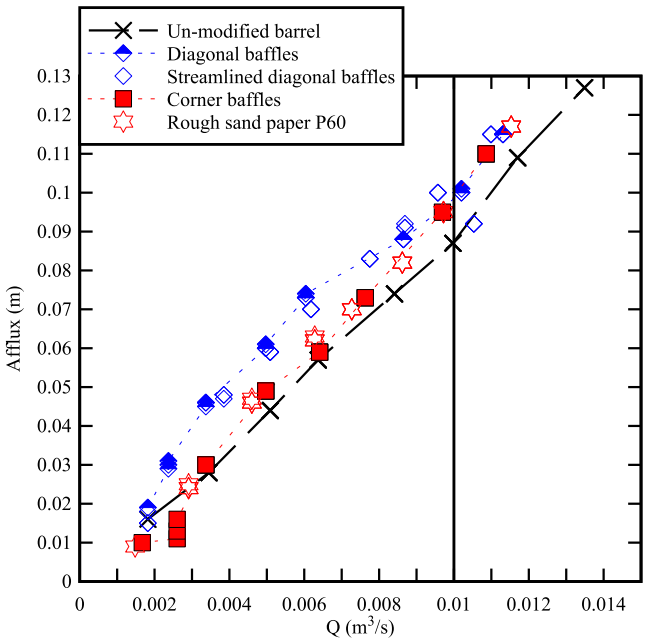

Fig. 5. Relationship between afflux and discharge for un-modified box culvert (thick dashed line and cross) and box culvert equipped with baffle designs (coloured symbols) – Solid vertical line corresponds to design discharge.

4. Secondary motion in rough boundary conditions

4.1. Presentation

During the experiments Series 2, detailed velocity measurements were conducted in the fully-developed flow region. Typical results are shown in Fig. 6 in terms of the time-averaged longitudinal velocity and standard deviation of velocity components for the rough bed and sidewall configuration. Owing to the presence of the free-surface and of differences in boundary friction along the wetted perimeter, the velocities in the channel were not uniformly distributed and the velocity field was not symmetrical about the channel centreline (Fig. 6A). This was evidenced with dye injection showing a slower flow motion next to the rough invert and next to the rough left sidewall, with complicated flow patterns next to the left corner. The time-averaged longitudinal velocity data showed a complicated velocity pattern in the left bottom corner with the rough bed and rough left sidewall. A phenomenon of velocity dip is seen in Fig. 6A, in which the maximum velocity V_{max} at each transverse location was observed at a vertical elevation $Z_{Vmax}/d < 1$, where d is the depth of flow. The dip in velocity profile was believed to be caused by the presence of secondary currents (Nezu and Rodi, 1985; Apelt and Xie, 2011). Low momentum fluid was transported from near the side walls to the centre and high momentum fluid was moved from the free surface toward the rough bed and sidewalls (Gibson, 1909; Nezu and Rodi, 1985; Xie, 1998). The maximum velocity and its location were found to be functions of the transverse locations (Fig. 7). Fig. 7 regroups experimental observations in fully-developed flows for both smooth and rough configurations, where B is the channel width and V_{mean} is cross-sectional averaged velocity: $V_{mean} = Q/(B \times d)$. For the rough bed and sidewall configuration, the cross sectional maximum velocity was observed in average at about $Z_{Vmax}/d \approx 0.62$ and $Y_{Vmax}/B = 1/3$, where $V_{max}/V_{mean} \approx 1.6$. That is, the cross-sectional maximum was observed below the free-surface towards the right smooth sidewall. The relative elevation of cross-sectional maximum velocity was close to the observations of Xie (1998) in a smooth channel: $Z_{Vmax}/d \approx 0.66$. On the channel centreline (y/B = 0.5), the ratio of maximum velocity to free-surface velocity equalled 1.03 on average. For comparison, Nezu and Rodi (1985) reported $V_{max}/V_{fs} \approx 1.1$ in a smooth and wide channel (B/d = 10). Close to the sidewalls, the ratio of maximum velocity to free-surface velocity was larger than or equal to 1.1, and the relative elevation of maximum velocity was within $Z_{Vmax}/d \approx 0.3–0.5$ (Fig. 7B).

Contours of distributions of velocity fluctuations v_x', v_y' and v_z' are shown in Fig. 6B–D. Maximum velocity fluctuations were recorded close to the rough bed and rough sidewall. (The rough sidewall is on the right of each graph.) Along most vertical lines away from side walls, the longitudinal velocity fluctuations v_x' presented a local minimum below the free surface, at about the same elevation where the longitudinal velocity V_x was maximum. From this local minimum, v_x' increased slightly towards the free surface and increased substantially with depth to its maximum close to the invert. (Theoretically, v_x', v_y' and v_z' should be zero at z = 0, but the lowest ADV sampling elevation was z = 0.0058 m.). The trend was also seen with the smooth bed data, and previously reported by Apelt and Xie (2011). The cross sectional minimum values of longitudinal velocity fluctuations were on about the centreline with $(v_x')_{min}/V_{mean} \sim 0.10–0.12$. The cross-sectional maximum value of $(v_x')_{max}/V_{mean}$ was observed close to the bottom left rough wall, with values about 1.6–2.0. Physically the magnitude of v_x' increased in regions where the velocity gradients $\partial V_x/\partial y$ and $\partial V_x/\partial z$ increased. The change in boundary roughness along the wetted perimeter affected these gradients and resulted in a re-distribution of turbulent kinetic energy. The boundary roughness change had a most significant effect on the turbulence intensity. The magnitude of velocity fluctuations was large near the rough sidewall across most of the water column, and it became much smaller near the channel centreline.

Contours of distributions of transverse and vertical velocity fluctuations, v_y' and v_z' respectively, are presented in Fig. 6C and D. Compared to the distributions of longitudinal velocity fluctuations, the data were similar except for the following differences. The vertical velocity fluctuation v_z' was reduced next to the free surface while v_x' was enhanced due to the water surface, as observed by Xie (1998). Another difference was the magnitudes of v_z', consistently larger than those of v_x'. The reason remains unclear but it might have been linked to the instrumentation. While it is hard to find precise data of the transverse velocity fluctuations v_y' in the literature, the present v_y' data in most parts away from solid boundaries of each cross section were small, consistently smaller than v_x'.

A comparison between the distributions of v_x' and v_y' suggested similar distribution patterns. Along most vertical lines away from sidewalls, the transverse velocity fluctuation v_y' had a local minimum below the free surface. This local minimum was located in the region where the time-averaged longitudinal velocity V_x was maximum. From this local minimum, v_y' increases towards the free surface and increased with depth to its maximum next to the channel bed. The minima of v_y' at all locations in the fully-developed flow region were about $(v_y')_{min}/V_{mean} \sim 0.05–0.07$ on average. Near the sidewalls, v_y' exhibited high values over most parts of the water column.

4.2. Discussion

Visual observations, supported with dye injection, showed some recirculation motion next to the left rough sidewall and at the corner between the rough bed and sidewall. A strong longitudinal vortex stretched near the channel bed and a smaller vortex took place on the left side near the free surface. No similar vortex pattern was seen on the right side of the channel, possibly because the transverse velocity gradient $\partial V_x/\partial y$ was large and

(A) Contour plot of constant longitudinal velocity V_x

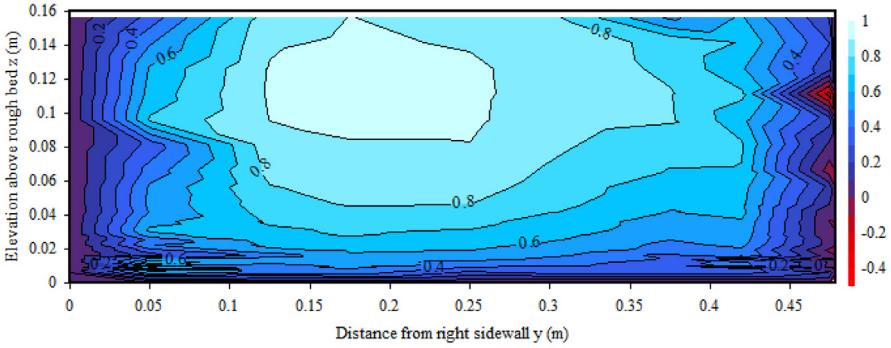

(B) Contour plot of constant longitudinal velocity fluctuations v_x'

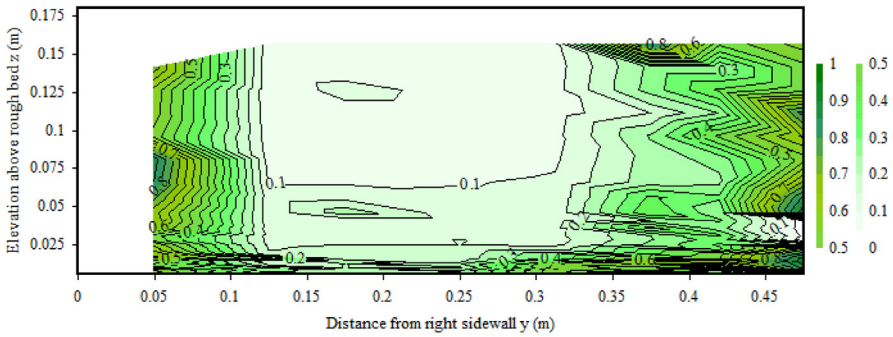

(C) Contour plot of constant transverse velocity fluctuations v_y'

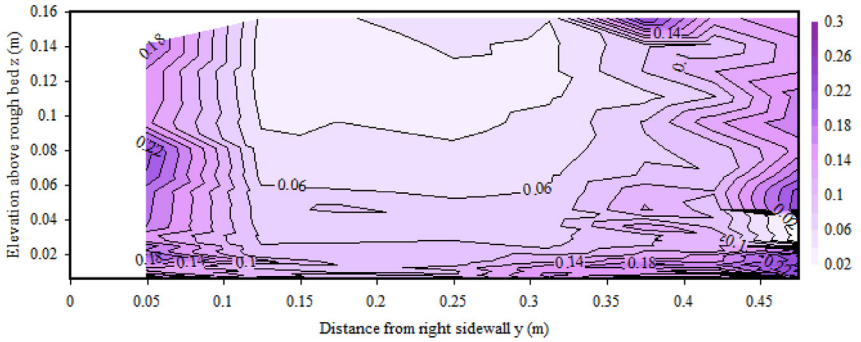

(D) Contour plot of constant vertical velocity fluctuations v_z'

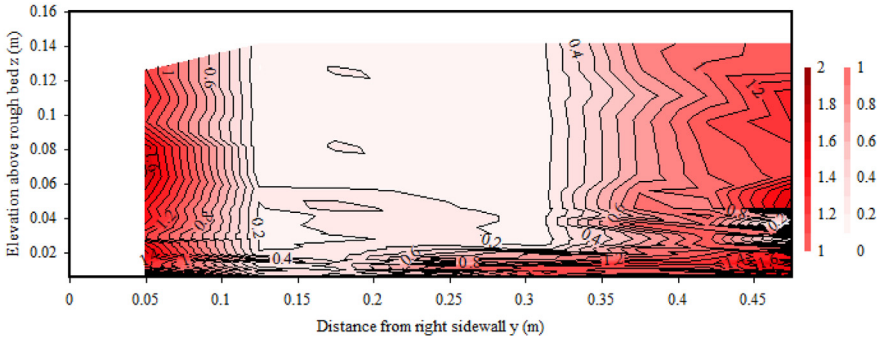

Fig. 6. Contour curves of constant longitudinal velocity V_x and velocity fluctuations v′ in the 12 m long channel with rough bed and sidewall – Q = 0.0556 m^3/s, x = 8 m, y = 0 at right smooth sidewall, velocity scale in m/s. (A) Contour plot of constant longitudinal velocity V_x. (B) Contour plot of constant longitudinal velocity fluctuations v_x'. (C) Contour plot of constant transverse velocity fluctuations v_y'. (D) Contour plot of constant vertical velocity fluctuations v_z'.

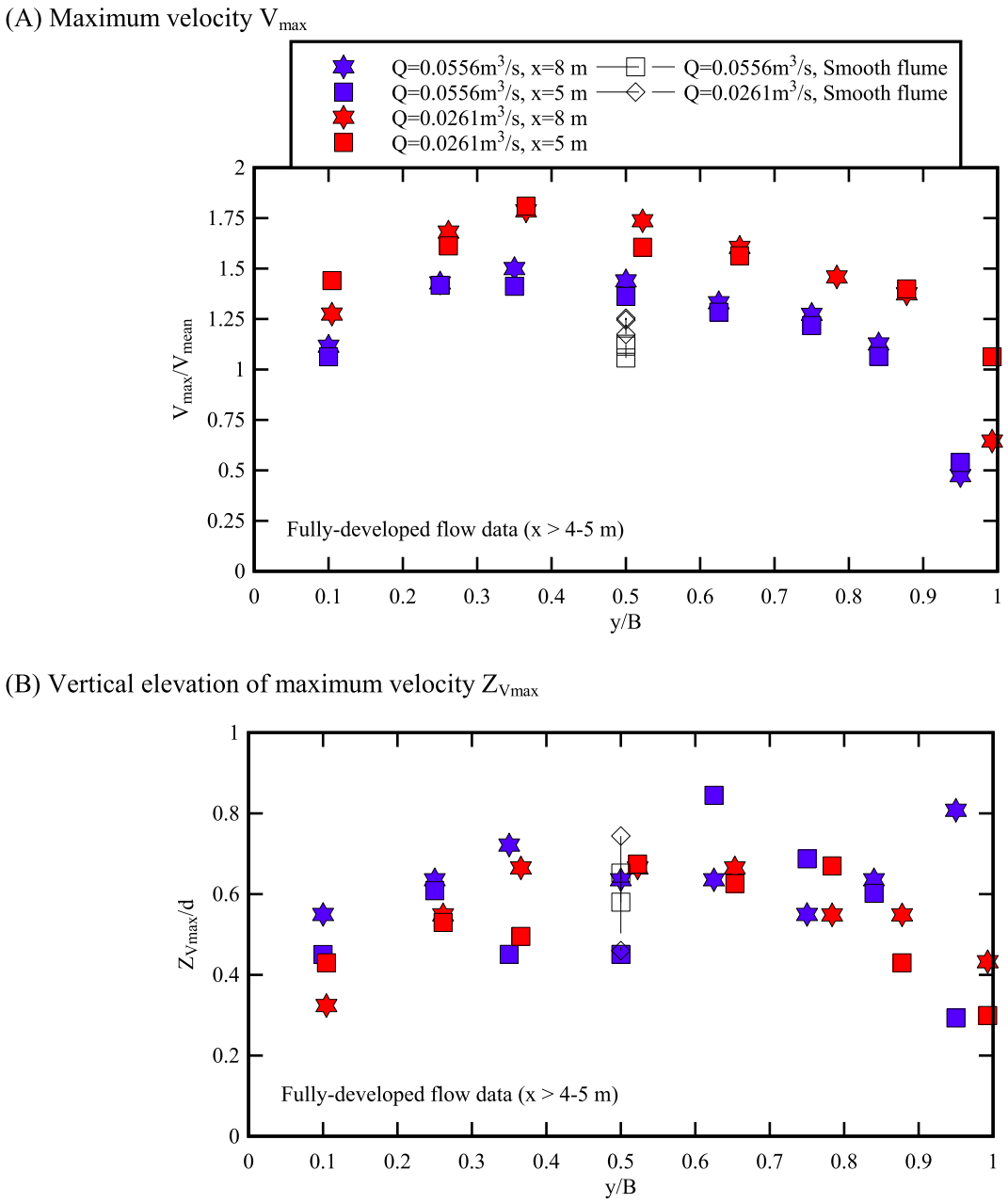

Fig. 7. Transverse distribution of maximum velocity and its vertical position as functions of the transverse location in the 12 m long channel with rough bed and sidewall, with the same legend for all graphs – Comparison with centreline data for smooth channel configuration – Note y = 0 at the right smooth sidewall. (A) Maximum velocity V_{max}. (B) Vertical elevation of maximum velocity Z_{Vmax}.

dye recirculation was not visible. These vortical structures are called 'bottom vortex' and 'free surface vortex' respectively (Apelt and Xie, 2011).

Several studies acknowledged that the turbulence in fish pass plays a key role in fish behaviour (Yasuda, 2011; Breton et al., 2013). Substrate roughening was observed to increase the likelihood of successful passage of small-bodied native Australian fish species (Heaslip, 2015). Nikora et al. (2003) hinted however the potential interplay between turbulence length scales and fish dimensions. More generally, culvert design guidelines recommend for regions of low velocities to assist with fish passage as well as for fish to rest and reduce lactic acid build-up, including for small-bodied fish (Boubee et al., 2000; Abbs et al., 2007). The same guidelines recommend the use of macro-roughness to improve fish passage in culverts (Boubee et al., 2000).

In the 12 m long flume with rough sidewall and invert, the percentage of the flow area with time-averaged velocities less than the bulk velocity V_{mean} was 45% in the fully-developed flow region, while 30% of the flow area experienced time-averaged velocities less than $0.75 \times V_{mean}$ and 17% of the flow area experienced time-averaged velocities less than $0.5 \times V_{mean}$ (Fig. 6A) These low velocity regions corresponded to large velocity fluctuations, especially the lower left corner (between rough wall and invert) where the longitudinal velocity standard deviation was greater than $v_x'/V_{mean} > 0.33$ (Fig. 6). These regions of low velocity and higher turbulence are preferential swimming zones for fish, as shown by Lupandin (2005) and Cotel et al. (2006), and could be favorable small-bodied fish passage, although further experiments involving detailed fish behaviour study are required for validation and guideline development.

5. Summary and discussion

A physical study of box culvert was performed under controlled flow conditions, and seven designs were tested. The study aimed to minimise the increase in afflux and to maximise slow flow, secondary current and recirculation regions, to facilitate the passage of fish with small body mass, in particular upstream migration. In all the cases, the turbulence of the flowing waters was used to enhance potential fish migration. In the box culvert model (Series 1), one configuration presented promising results: i.e., small corner baffles. The corner baffle system produced little additional afflux, while creating excellent recirculation both upstream and downstream of each baffle. The resulting flow conditions maybe more favorable to the passage of small-bodied fish typical in Australian streams.

Another configuration (Series 2) consisted of a very rough bed plus a very rough sidewall and a smooth sidewall. The analysis of the results showed an asymmetrical velocity field, the existence of the velocity dip and the presence of secondary currents in the three-dimensional turbulent flows. Visual observations and dye injection indicated a recirculation motion next to the left rough sidewall and at the corner between the rough bed and sidewall. The maximum velocity and its location were found to be functions of the transverse locations. The cross-sectional maximum was observed below the free-surface towards the right smooth sidewall. The relative elevation of cross-sectional maximum velocity was close to past observations in smooth channels. Maximum velocity fluctuations were recorded close to the rough bed and rough sidewall. This rough boundary configuration appeared to provide excellent recirculation regions next to the rough sidewall and at the corner between the rough sidewall and channel bed, which might be suitable to the upstream passage of small fish, typical of Australian native species.

It must be acknowledged that the present findings are preliminary. Further design testing must be conducted to develop quantitative design guidelines, in terms of optimum baffle dimensions and spacing (corner baffles), and boundary roughness (rough bed and sidewall). Tests must further encompass impact on real fish passage: that is, using fish-friendly laboratory facilities, to be complemented by field monitoring of prototype structures.

Acknowledgments

HC acknowledges the experimental work of his students Urvisha Kiri, Caitlyn Johnson and Laura Beckingham (The University of Queensland). The authors acknowledge the technical assistance of Jason Van Der Gevel and Stewart Matthews (The University of Queensland). HC acknowledges helpful discussions with Dr Matthew Gordos and his NSW Department of Fisheries colleagues, and the input of Prof Craig Franklin (The University of Queensland). The authors thank the reviewers for their helpful comments. The financial support through the Australian Research Council (Grant LP140100225) is acknowledged.

References

Abbs, T.J., Kells, J.A., Katapodis, C., 2007. A model study of the hydraulics related to fish passage through backwatered culverts. In: Proc. 18th Canadian Hydrotechnical Conference, Winnipeg, Manitoba, 22024 August, 13 pages.

Apelt, C.J., Xie, Q., 2011. Measurements of the turbulent velocity field in a non-uniform open channel. In: Eric Valentine, Colin Apelt, James Ball, Hubert Chanson, Ron Cox, Rob Ettema, George Kuczera, Martin Lambert, Bruce Melville, Jane Sargison (Eds.), Proc. 34th IAHR World Congress, Brisbane, Australia, 26 June-1 July, Engineers Australia Publication, pp. 3338–3345 (ISBN 978-0-85825-868-6).

ASCE, 1942. Hydraulic Models. American Society of Civil Engineers, Manual of Engineering Practice No. 25, 110 pages.

Baker, C.O., Votapka, F.E., 1990. Fish passage through culverts. Dept. of Transportation, Federal Highway Administration, United States Department of Agriculture, Forest Service, Washington, D.C., USA.

Boubee, J., Williams, E., Richardson, J., 2000. Fish passage guidelines for the Auckland Region. Auckland Regional Council, Technical Publication No. 131, 50 pages.

Breton, F., Baki, A.B.M., Link, O., Zhu, D.Z., Rajaratnam, N., 2013. Flow in nature-like fishway and its relation to fish behaviour. Can. J. Civ. Eng. 40, 567–573.

Brigg, A.S., Galarowicz, T.L., 2013. Fish passage through culverts in central Michigan warmwater streams. North Am. J. Fish. Manag. 33, 652–664.

Chanson, H., 1999. The Hydraulics of Open Channel Flow: An Introduction. Edward Arnold, London, UK. 512 pages.

Chanson, H., 2004. The Hydraulics of Open Channel Flow: An Introduction. Butterworth-Heinemann, Oxford, UK. 630 pages (ISBN 978 0 7506 5978 9).

Chanson, H., Uys, W., 2016. Baffle designs to facilitate fish passage in box culverts: a preliminary study. In: Crookston, B., Tullis B. (Eds.), Proceedings of 6th IAHR International Symposium on Hydraulic Structures, Hydraulic Structures and Water System Management, 27–30 June, Portland OR, USA, pp. 295–304. doi: 10.15142/T300628160828.

Cotel, A.J., Webb, P.W., Trittico, H., 2006. Do brown trout choose locations with reduced turbulence? Trans. Am. Fish. Soc. 135, 610–619.

Djenidi, L., Elavarasan, R., Antonia, R.A., 1999. The turbulent boundary layer over transverse square cavities. J. Fluid Mech. 395, 271–294.

Fairfull, S., Witheridge, G., 2003. Why do fish need to cross the road? Fish passage requirements for waterway crossings. NSW Fisheries, Cronulla NSW, Australia, 14 pages.

Gibson, A.H., 1909. On the depression of the filament of maximum velocity in a stream flowing through an open channel. Proc. R. Soc. London Ser. A 82, 149–159.

Heaslip, B.M., 2015. Substrate Roughnening Improves Swimming Performance of Two Small bodied Riverine Fish Species: Implications for Culvert Design. Honours thesis, The University of Queensland, School of Biological Sciences, Brisbane, Australia, 32 pages.

Hee, M., 1969. Hydraulics of culvert design including constant energy concept. In: Proc. 20th Conf. of Local Authority Engineers, Dept. of Local Govt, Queensland, Australia, paper 9, pp. 1–27.

Henderson, F.M., 1966. Open Channel Flow. MacMillan Company, New York, USA.

Hotchkiss, R., 2002. Turbulence investigation and reproduction for assisting downstream migrating juvenile salmonids, Part I. BPA Report DOE/BP-00004633-I, Bonneville Power administration, Portland, Oregon, 138 pages.

Larinier, M., 2002. Fish Passage through Culverts, Rock Weirs and Estuarine Obstructions. Bull. Fr. Pêche Piscic. 364 (18), 119–134.

Liao, J.C., Beal, D.N., Lauder, G.V., Triantafyllou, M.S., 2003. The Kármán gait: novel body kinematics of rainbow trout swimming in a vortex street. J. Exp. Biol. 206, 1059–1073. http://dx.doi.org/10.1242/jeb.00209.

Liu, M.M., Rajaratnam, N., Zhu, D.Z., 2006. Mean flow and turbulence structure in vertical slot fishways. J. Hydraulic Eng., ASCE 139 (4), 424–432.

Lupandin, A.I., 2005. Effect of flow turbulence on swimming speed of fish. Biol. Bull. 32 (5), 461–466.

Nezu, I., Rodi, W., 1985. Experimental study on secondary currents in open channel flow. In: Proceedings 21st IAHR Biennial Congress, Melbourne, Australia, pp. 114–119.

Nikora, V.I., Aberle, J., Biggs, B.J.F., Jowett, I.G., Sykes, J.R.E., 2003. Effects of fish size, time-to-fatigue and turbulence on swimming performance: a case study of *Galaxias Maculatus*. J. Fish Biol. 63, 1365–1382.

Novak, P., Cabelka, J., 1981. Models in Hydraulic Engineering. Physical Principles and Design Applications. Pitman Publ., London, UK. 459 pages.

Novak, P., Moffat, A.I.B., Nalluri, C., Narayanan, R., 2001. Hydraulic Structures. Spon Press, London, UK. 666 pages.

Olsen, A., Tullis, B., 2013. Laboratory study of fish passage and discharge capacity in slip-lined, baffled culverts. J. Hydraulic Eng., ASCE 139 (4), 424–432.

Papanicolaou, A.N., Talebbeydokhti, N., 2002. Discussion of "Turbulent open-channel flow in circular corrugated culverts". J. Hydraulic Eng., ASCE 128 (5), 548–549.

Pavlov, D.S., Lupandin, I.A., Skorobogatov, M.A., 2000. The effects of flow turbulence on the behavior and distribution of fish. Jl Ichthyol 40, S232–S261.

Pfister, M., Chanson, H., 2012. Scale effects in physical hydraulic engineering models. Discussion. J. Hydraulic Res., IAHR 50 (2), 244–246. http://dx.doi.org/10.1080/00221686.2012.654672.

Wang, R.W., David, L., Larinier, M., 2010. Contribution of experimental fluid mechanics to the design of vertical slot fish passes. Knowl Manag Aquat Ecosyst, vol. 396, No. 02, 21 pages.

Wang, H., Beckingham, L.K., Johnson, C.Z., Kiri, U.R., Chanson, H., 2016. Interactions between Large Boundary Roughness and High Inflow Turbulence in Open channel: a Physical Study into Turbulence Properties to Enhance Upstream Fish Migration. Hydraulic Model Report No. CH103/16, School of Civil Engineering, The University of Queensland, Brisbane, Australia, 74 pages (ISBN 978-1-74272-156-9).

Warren Jr., M.L., Pardew, M.G., 1998. Road crossings as barriers to small-stream fish movement. Trans. Am. Fish. Soc. 127, 637–644.

Washington Mills, 2015. Grit Sizes: Particle Size Conversion Chart – ANSI. <http://www.washingtonmills.com/guides/grit-sizes-ansi/particle-size-conversion-chart-ansi/> (Retrieved 5th June, 2015)

Yasuda, Y., 2011. Guideline of Fishway for Engineers. Corona Publishing, NPO Society for Fishway in Hokkaido, Japan, 154 pages (in Japanese).

Xie, Q., 1998. Turbulent Flows in Non-Uniform Open Channels: Experimental Measurements and Numerical Modelling. Ph.D. thesis, Dept. of Civil Engineering, University Of Queensland, Australia, 339 pages.

Webb, P.W., Cotel, A.J., 2011. Stability and Turbulence. Encyclopaedia of Fish Physiology: from Genome to Environment, vol. 1–3, pp. 581–586. doi: 10.1016/B978-0-12-374553-8.00221-5.